Magnetic properties of Ni clusters embedded in AlN by x-ray magnetic circular dichroism

1998 J. Phys.: Condens. Matter 10 9721

(http://iopscience.iop.org/0953-8984/10/43/015)

J. Phys.: Condens. Matter **10** (1998) 9721–9727. Printed in the UK PII: S0953-8984(98)93561-5

Magnetic properties of Ni clusters embedded in AlN by x-ray magnetic circular dichroism

D Zanghi†, A Delobbe, A Traverse and G Krill

Laboratoire LURE, Centre Universitaire Paris-Sud, Bâtiment 209A, BP 34, 91898 Orsay Cédex, France

Received 22 April 1998, in final form 2 July 1998

Abstract. Magnetic Ni clusters, with an average diameter of 1.9 nm, were prepared by ion implantation in a sintered AlN matrix. X-ray magnetic circular dichroism measurements were performed on this sample at 100 K and 300 K, by measuring the $L_{2,3}$ edges of Ni under a magnetic field of ± 0.6 T. Using the sum rules currently applied to the bulk transition metals, we deduce a total magnetic moment and the orbital and spin contributions to this moment. The magnetic moment is in good agreement with the values measured by SQUID magnetometry at the same temperatures.

1. Introduction

The major part of the experimental and theorical work in the field of cluster magnetism has been dedicated to the study of transition metals.

These small particles are known to display physical, electronic and magnetic properties different from those of the corresponding bulk materials, for instance the increase of magnetic moment [1, 2], a superparamagnetic behaviour [3, 4] and giant magnetoresistance [5, 6]. From a fundamental point of view, clusters help to understand how the magnetic behaviour evolves as one reduces the cluster size below the single-domain size.

To follow this evolution x-ray magnetic circular dichroism (XMCD) is complementary to SQUID magnetometry, with a better selectivity with regards to the atomic species and the symmetry of the contributing magnetic states. The dichroic signal is the difference between the absorption spectra measured with circularly polarized radiation when the magnetic field is applied along the x-ray wavevector direction and in the reverse direction. Another possibility is to reverse the photon helicity. Thanks to the sum rules applied to the dichroic signal, the average values of the orbital and spin contributions to the total magnetic moment can be deduced, allowing one to correlate the electronic properties to the magnetic ones.

One of the sum rule relates the integrated dichroic signal to the value of the operator $\langle L_z \rangle$ associated with the ground state orbital moment of the electronic shell probed by the photoelectron [7]. The second sum rule, which can be applied to $L_{2,3}$ and $M_{4,5}$ edges, relates a linear combination of the XMCD signals to the two operators $\langle S_z \rangle$ and $\langle T_z \rangle$ which represent the spin part of the magnetic moment and the shape of the spin asymmetry (magnetic dipole operator) [8]. The z axis is taken as the direction of the applied magnetic field (sufficiently large to magnetically saturate the sample). In the case of measurements at $L_{2,3}$ edges ($2p \rightarrow 3d$ transitions) the orbital and spin magnetic moments, are given by

† Contact author; e-mail: ZANGHI@lure.u-psud.fr.

0953-8984/98/439721+07$19.50

the relationships $m_{orb} = -\langle L_z \rangle \mu_b$ and $m_{spin} = -2\langle S_z \rangle \mu_b$. The total magnetic moment is thus: $m = m_{spin} + m_{orb}$ [9, 10].

It is now well established that one can apply these sum rules to bulk materials and thin films of transition metals [11, 12]. Two difficulties arise in the applicability of the XMCD sum rules to clusters. The first one concerns the fact that the number of holes in the final state (3d shell for example) has to be known to deduce $\langle L_z \rangle$. The number of holes is expected to vary as compared to the bulk value: this is due to a modification of the electronic density of states particularly on atoms located at the cluster surface. This n_h value is not known *a priori*. The second difficulty concerns $\langle T_z \rangle$. The general rule is that $\langle T_z \rangle = 0$ in a cubic crystal field without spin–orbit coupling. For several cases, taking into account spin–orbit coupling may lead to large value of $\langle T_z \rangle$ at low temperature [13–15]. However, at 100 K and 300 K, the spin–orbit effects are quenched by the temperature effect so that it is reasonable to consider that $\langle T_z \rangle = 0$ in this case.

We present here measurements of the $L_{2,3}$ edges and the dichroic signal for Ni clusters of 1.9 nm diameter, an intermediate situation between bulk and very small particles. To deduce the m_{orb} and m_{spin} values, we considered, as for bulk Ni, that $n_h = 0.54$ [9] and $\langle T_z \rangle = 0$. The total magnetic moment obtained from absorption and XMCD data was compared to the value measured by a SQUID magnetometer. The good agreement between both results confirms the validity of our assumptions concerning n_h and $\langle T_z \rangle$.

These are preliminary XMCD measurements on clusters embedded in a ceramic matrix. To our knowledge, very little work has been reported in this field.

2. Experimental details

2.1. Sample preparation and characterization

The AlN bulk sample used in the present study is produced by powder sintering. The sample was implanted with 80 keV Ni^+ on the low energy ion implanter IRMA of the Centre de Spectrométrie Nucléaire et de Spectrométrie de Masse (CSNSM) at Orsay, France [16]. The implanted fluence was 1.03×10^{17} ions cm^{-2}. After implantation, in order to recover the AlN matrix from defects introduced during implantation, the sample was annealed at 800 °C for one hour under a vacuum of the order of 10^{-4} Pa.

The depth profile and the atomic concentration were measured by Rutherford backscattering spectroscopy (RBS) using 1.5 MeV He^+ ions on the tandem Van de Graaff accelerator ARAMIS of the CSNSM [17].

Comparison of the RBS spectra of the as-implanted sample with the post-annealed sample indicates that the thermal treatment causes a loss of Ni atoms (7%) from the matrix. The narrowing of the impurity profile accompanied by an increase of the maximum concentration after annealing can be attributed to an Oswald ripening process. The concentration profile of the post-annealed sample is homogeneous up to a depth of around 60 nm from the surface. The fluence 1.03×10^{17} ions cm^{-2} corresponds to an average Ni concentration of 14% in this area.

We used x-ray absorption spectroscopy (XAS) to identify Ni cluster formation. The x-ray absorption spectra were recorded at beamline D42 of the DCI storage ring of the LURE synchrotron. The absorption curves at the Ni K edge (8333 eV) were collected in a total electron yield (TEY) detection mode at liquid nitrogen temperature. Experimental details have been described elsewhere [18].

The experimental EXAFS (extended x-ray absorption fine structure) oscillations were Fourier transformed to obtain a pseudoradial function (PRF). The oscillations of the Fourier

Table 1. Structural results from XAS experiments.

Fluence (at cm^{-2})	$\bar{N}_1$	$\bar{R}_1$ (nm)	$\bar{D}$ (nm)
1.03×10^{17}	9.6 ± 0.5	0.249 ± 0.001	1.9 ± 0.4

transform for the implanted sample display similar features to those observed in Ni metal, but with less intensity. Analysis of the EXAFS oscillations led us to conclude that Ni atoms are surrounded by Ni after the collision cascade. The implanted Ni ions precipitated in the matrix to form Ni fcc clusters [19].

By fitting the first peak of the PRF, we obtain the number (N) and the distances (R) of atoms in the neighbouring shells of the probed atom. By using the approximated formula for spherical particles [20]: $N_n(D) = N_n^{bulk}(1 - 3R_n/2D)$ where R_n is the nth shell radius, D is the average diameter of the cluster, N_n is the nth shell coordination number, we can determine the size of the clusters. The results are presented in table 1.

2.2. Magnetic measurements

2.2.1. SQUID measurements The magnetization measurements were performed at the Laboratoire de Physique des Matériaux de Nancy (France), using a commercial SQUID (superconducting quantum interference device) magnetometer made by quantum design ($H_{max} = \pm 7$ T, $T_{max} = 400$ K).

The measurements at different temperatures (5, 100, 300 K) were performed with the sample oriented parallel and perpendicular to the direction of the magnetic field in the range of ± 4 T. The sample was ground down to a thickness of 120 μm in order to reduce the magnetic signal from the matrix. To separate the diamagnetic contribution of the matrix from the ferromagnetic contribution (possibly superparamagnetic at high temperature) of the Ni clusters, we subtracted from the total signal, the signal of a sample from which the implanted layer has been removed.

2.2.2. XMCD measurements. The experiments were carried out at beamline SU22 of the Super ACO storage ring of the LURE synchrotron operating with currents of 100–400 mA in a 24 bunch mode. We used a double crystal Be($10\bar{1}0$) monochromator with a resolution of 0.26 eV at 850 eV.

The x-ray absorption spectra were performed at the Ni $L_{2,3}$ edges in TEY detection mode. The data were collected by measuring the sample current in the range 0.1–1.2 pA depending on the Ni sample (foil or clusters). The probing depth of the TEY is estimated to be in the 2.5 nm range at the $L_{2,3}$ edges of Ni [21]. This means that the information is representative of the near surface region and the number of Ni atoms probed in the sample is weak (4×10^{15} ions cm^{-2}, equivalent to four monolayers). Moreover, as the mean diameter of the clusters is smaller than the probing depth, we assume that the collected information is representative of the whole clusters and not of part of them.

For these measurements, the photon incident angle with the surface normal of the sample was set at 0°. The degree of circular polarization is estimated to be 30%. The XMCD data were obtained by alternating the applied magnetic field ($H = \pm 0.6$ T for the sample and ± 1 T for the Ni foil) at each photon energy with a frequency of about 1 Hz. The sample was placed perpendicular to the direction of the magnetic field. Measurements were taken at 100 K and 300 K; unfortunately no measurement at 5 K was performed.

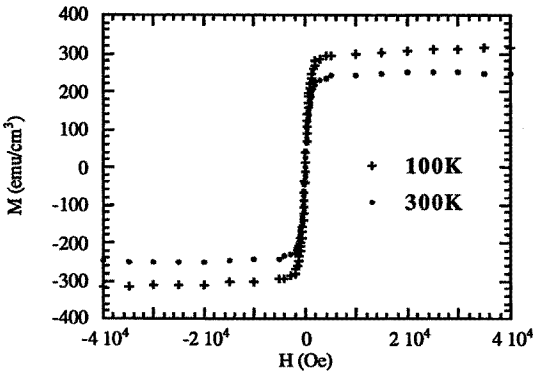

Figure 1. Magnetization versus perpendicular field at 100 K and 300 K for the implanted sample.

Table 2. SQUID measurements: magnetic moment for $H = \pm 0.5$ T.

T (K)	M (emu cm^{-3})	M (μ_b/atom)
100	306 ± 4	0.361 ± 0.005
300	247 ± 8	0.29 ± 0.01

3. Results and discussion

3.1. SQUID measurements

The magnetization M versus field was measured at several temperatures (figure 1). The values for $H = \pm 0.5$ T are listed in table 2. In order to calculate the magnetic moment per atom we used the number of atoms measured by RBS. At low temperature ($T = 5$ K) the saturation magnetization is close to the bulk value (0.6 μ_b/atom). It is the same value obtained by Billas and coworkers [1] for free Ni clusters of similar average diameter. It is only for smaller Ni clusters that the magnetic moment increases. Such a magnetic moment value close to 0.6 μ_b/atom also indicates that there is no antiferromagnetic coupling between the clusters in AlN. For higher temperature, 100 K and 300 K, we observed a decrease in the magnetic moment due to a superparamagnetic behaviour [4], as expected for small particles. A blocking temperature of 60 K, which marks the border between a well ordered state and a superparamagnetic one, was deduced from zero-field-cooled and field-cooled curves (not shown here) under a magnetic field of 0.01 T.

3.2. XMCD measurements

Figure 2 displays the absorption and the XMCD spectra (normalized to 100% of circular polarization rate) for the AlN/Ni sample annealed and for a Ni foil.

In order to minimize the problem of the surface oxidation, the Ni foil has been scraped *in situ* with a diamond file. For the implanted sample, this procedure was not necessary because the clusters, which are under the surface, are not contaminated by oxygen. This is confirmed by the examination of the absorption spectra. The absence of a shoulder at the L_3 edge and a double feature at L_2 edge, characteristic of a NiO compound, proves that the clusters are not oxidized over the region probed. Moreover, the great similarity between

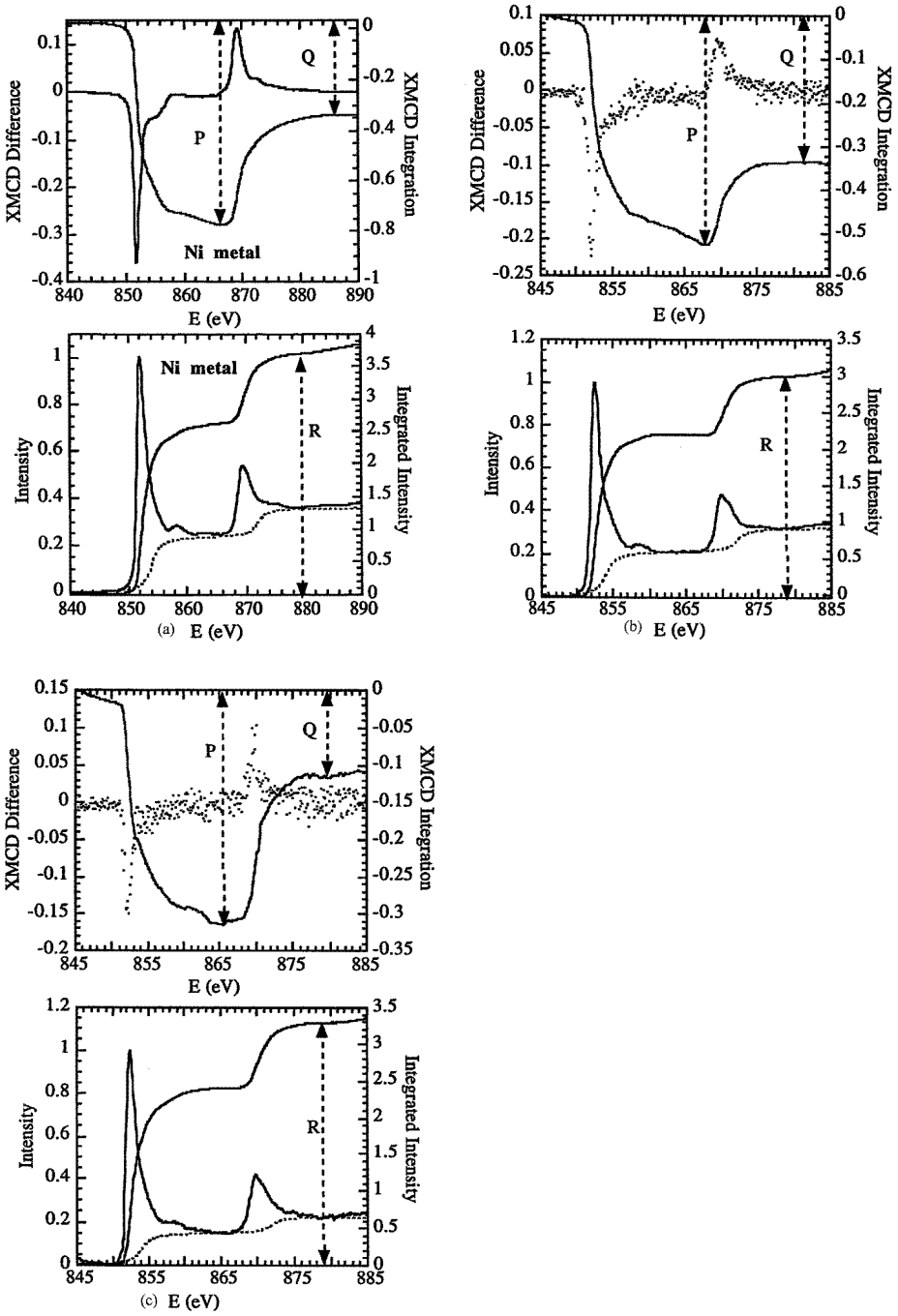

Figure 2. (a) Absorption and XMCD spectra (normalized to 100% of circular polarization rate) obtained for $L_{2,3}$ edges of Ni metal. (b) Absorption and XMCD spectra (normalized to 100% of circular polarization rate) obtained for $L_{2,3}$ edges of the implanted sample, recorded at $H = \pm 0.6$ T and $T = 100$ K. (c) Absorption and XMCD spectra (normalized to 100% of circular polarization rate) obtained for $L_{2,3}$ edges of the implanted sample, recorded at $H = \pm 0.6$ T and $T = 300$ K.

the shapes of $L_{2,3}$ signals for the Ni foil and for our sample, whatever the temperature, indicates that overwhelming modifications appear neither in the electronic distribution nor in the crystal field symmetry. This supports our choice of $n_h = 0.54$ and $\langle T_z \rangle = 0$ together with our assumption that surface effects are negligible.

According to the sum rules, the orbital and spin magnetic moments are given by $m_{orb} = -(2Q/3R)n_h$ and $m_{spin} = -[(3P - 2Q)/R]n_h$ where P is the dichroic signal integrated over the L_3 edge, Q is the dichroic signal integrated over the $L_{2,3}$ edges. R is the integral of the absorption spectrum after subtraction of a double step function. The spectra for the foil and the clusters have been treated in exactly the same way, following the procedure indicated by Arvanitis *et al* [22]. The integrals P, Q, R are represented in figure 2. m_{orb} and m_{spin} are calculated taking $n_h = 0.54$. Values for P, Q, R, m_{orb} and m_{spin}, and the total magnetic moment, m, are presented in table 3 for an Ni foil and the implanted sample.

Table 3. Results of the XMCD experiments performed at $H = \pm 1$ T for the Ni foil and $H = \pm 0.6$ T for the implanted sample. The magnetic moments are given in μ_b/atom.

	$-P$	$-Q$	R	m_{orb}	m_{spin}	$\frac{m_{orb}}{m_{spin}}$	m
Ni metal $T = 10$ K	0.78	0.34	3.7	3.3×10^{-2}	0.24	0.13	0.51
Ni/AlN $T = 100$ K	0.51	0.31	2.84	3.9×10^{-2}	0.17	0.23	0.38
Ni/AlN $T = 300$ K	0.31	0.12	3.34	1.3×10^{-2}	0.11	0.11	0.23

For the Ni foil, a magnetic moment equal to 0.51 μ_b/atom is found. The difference between this value and the expected value for the bulk material (0.6 μ_b/atom) can be attributed to the n_h value used, the uncertainties in the degree of circular polarization of the incident photons or a slight oxidation at the surface. It remains that this gives credence to our measurements for both types of sample. Moreover the ratio m_{orb}/m_{spin} is in good agreement with the calculation given in [23].

Though the signal-to-noise ratio is rather large, the agreement between the value of the magnetic moment calculated by using the XMCD sum rules with the macroscopic value obtained by SQUID measurements for $H = \pm 0.5$ T is satisfactory. Even if the degree of circular polarization is slightly modified to rescale the magnetic moment of the Ni foil to 0.6 μ_b/atom (instead of 0.51 μ_b/atom), the new values for the cluster magnetic moment are increased by only 15%, which remains in agreement with the SQUID values to within the experimental uncertainties. This agreement confirms also the non-oxidized state of the clusters.

We note that the integral R, related to the number of 3d holes, is slightly smaller in the clusters as compared to the bulk. This indicates that the electronic distribution is already slightly different due to the cluster size.

Because the measurements were performed above the blocking temperature, hence in the superparamagnetic state, the total magnetic moment is weaker in the sample than in the bulk. Moreover the values of m_{orb} and m_{spin} decrease when the temperature increases. As in the bulk material the orbital moment is reduced by about one order of magnitude with regards to the spin moment. This small value indicates that the crystal field effects are not insignificant even for clusters of the measured size. The spin contribution to the total moment dominates.

The magnetic behaviour of these Ni clusters, either observed by XMCD or by SQUID magnetometry, is as expected taking into account their average size. However a different behaviour was reported by Eastham *et al* [24]. Via XMCD they show the decrease of the total magnetic moment of Co clusters embedded in a Cu matrix when the diameter increases. They interpret this as due to an antiferromagnetic exchange coupling between the clusters, unlike the situation in the AlN matrix. A key to understand these results might be in the unexpectedly large value of the m_{orb}/m_{spin} ratio which can be reached only by XMCD.

These different experiments prove that XMCD is a powerful technique to study magnetism of clusters. By probing directly the 3d electrons responsible for magnetism on a microscopic scale, this new technique offers the opportunity for studying how the magnetic properties change as the localized electrons of an isolated atom start to delocalize over several atoms.

However, the applicability of the XMCD rules still remain to be verified for smaller clusters where the surface effects are more important and can modify both the values of n_h and T_z. In this case a precise knowledge of these parameters by calculations is absolutely necessary for utilizing the sum rules.

Acknowledgments

We thank the ARAMIS/IRMA staff at CSNSM for the ion implantation and the technical staff of the beamline D42 at LURE for help during the experiments. We acknowledge C Bellouard and H Fischer for performing SQUID measurements.

References

[1] Billas I M L, Châtelain A and de Heer W A 1994 *Science* **265** 1682
[2] Reuse F A and Khanna S N 1995 *Chem. Phys. Lett.* **234** 77
[3] Bean C P 1955 *J. Appl. Phys.* **26** 1381
[4] Dormann J L 1981 *Rev. Phys. Appl.* **16** 275
[5] Berkowitz A, Young A P, Mitchell J R, Zang S, Carey M J, Spada F E, Parker F T, Hutten A and Thomas G 1992 *Phys. Rev. Lett.* **68** 3745
[6] Xiao J G, Jiang J S and Chien C L 1992 *Phys. Rev. Lett.* **68** 3749
[7] Thole B T, Carra P, Sette F and Van der Laan G 1992 *Phys. Rev. Lett.* **68** 1943
[8] Carra P, Thole B T, Altarelli M and Wang X 1993 *Phys. Rev. Lett.* **70** 694
[9] Kittel C 1983 *Physique de l'Ètat Solide* (Paris: Dunod) p 466
[10] Shore B W and Menzel D H 1968 *Principles of Atomic Spectra* (New York: Wiley)
[11] Wu R, Wang D and Freeman A J 1993 *Phys. Rev. Lett.* **71** 3581
[12] Chen C T, Idzerda Y U, Lin H J, Smith N V, Meigs G, Chaban E, Ho G H, Pellegrin E and Sette F 1995 *Phys. Rev. Lett.* **75** 152
[13] Crocombette J P, Thole B T and Jollet F 1996 *J. Phys.: Condens. Matter* **8** 4095
[14] Arrio M A, Sainctavit P, Brouder C and Deudon C 1995 *Physica* B **27** 208–9
[15] Sainctavit P, Arrio M A and Brouder C 1995 *Phys. Rev.* B **52** 12 766
[16] Chaumont J, Lalu F, Salomé M and Lamoise A M 1981 *Nucl. Instrum. Methods* **189** 193
[17] Bernas H *et al* 1992 *Nucl. Instrum. Methods* B **62** 416
[18] Traverse A, Zanghi D, Fischer H and Bellouard C 1997 *Proc. 5th Workshop on Non-crystalline Solids (Santiago de Compostela 1997)*
[19] Traverse A 1997 *Hyperfine Interact.* **110** 159
[20] Borowski M 1997 *J. Physique Coll.* IV **7** C2 259
[21] Stöhr J and Nakajima R 1997 *J. Physique Coll.* IV **7** C2 47
[22] Arvanitis D, Tischer M, Hunter Dunn J, May F, Martensson N and Baberschke K 1995 *Spin–Orbit-Influenced Spectroscopies of Magnetic Solids* vol 145, ed H Ebert and G Schütz (Berlin: Springer)
[23] Carra P 1993 *J. Appl. Phys.* **32** 279
[24] Eastham D A, Qiang Y, Maddock T H, Kraft J, Schille J-P, Thompson G S and Haberland H 1997 *J. Phys.: Condens. Matter* **9** L497